

## Feasibility study and stress analysis of friction stir extruded rods and pipes: a simulative model

Sara Bocchi<sup>1,a,\*</sup>, Cristian Cappellini<sup>1,b</sup>, Gianluca D'Urso<sup>1,c</sup>  
and Claudio Giardini<sup>1,d</sup>

<sup>1</sup> University of Bergamo - Department of Management, Information and Production Engineering,  
via Pasubio 7b, Dalmine (BG), 24044, Italy

<sup>a</sup>sara.bocchi@unibg.it, <sup>b</sup>cristian.cappellini@unibg.it, <sup>c</sup>gianluca.d-urso@unibg.it,  
<sup>d</sup>claudio.giardini@unibg.it

**Keywords:** Sustainable Processes, Aluminium Alloys, Friction Stir Extrusion

**Abstract.** The traditional aluminium recycling process consumes a lot of energy and adversely affects the metallurgical quality of the secondary alloys produced. With the increasing need for resolving this problem, Friction Stir Extrusion (FSE) has been patented. FSE is a new solid-state recycling process through which parts can be extruded directly from waste. In this research, the analysis was focused on different process parameters, process set ups and geometries of the extruded parts. The traditional setup, where the tool rotates and advances while the chamber remains stationary, was considered, and a new one was introduced. In this configuration, the tool has only an advance feed, while rotation is performed through the chamber. Moreover, for each combination of process parameters the bonding phenomena occurrence, considering both the thermal and the stress conditions generated by the parameters, was analysed. For this purpose, the Piwnik and Plata criterion was chosen.

### Introduction

The process of recycling aluminium traditionally involves re-melting scraps, forming new ingots, and reworking them into new billets for extrusion. Unfortunately, this process is highly energy-intensive due to the necessary combustion process, which also negatively affects the metallurgical quality of the secondary aluminium alloys obtained. Moreover, it is very difficult to completely eliminate all impurities from the aluminium bulk, which further compounds the problem [1].

Given the needs of a modern and sustainable industry, traditional recycling technologies have so far proved insufficient. The Friction Stir Extrusion (FSE) is a new solid-state recycling process that enables the direct extrusion of pieces from scraps, bypassing the most energy-intensive phases of traditional recycling. During the FSE process, a rotating tool is plunged into a hollow chamber to compact, stir, and back-extrude the scraps into a full, dense rod.

The FSE process is not limited to aluminium, either; it has been demonstrated in literature that it is also possible to use the FSE process to process magnesium and its alloys, including biodegradable ones [2], as well as dissimilar metals like aluminium and steel [3].

The innovation behind FSE lies in the use of heat developed exclusively through friction between the scraps and the tool: this leads to a reduced energy requirement of approximately 15% compared to traditional recycling technologies [4].

Despite its many benefits, the use of FSE in the industrial field is still limited due to the challenging correlation between process parameters and the final characteristics of the piece obtained, as well as the limitation of extrudable geometries. Currently, only axisymmetric pieces with diameters around ten millimetres can be obtained, because of to the complexity of predicting the behaviour of the chips in contact with each other, which leads to mechanical characteristics that limit the possibility of extruding large pieces.



As FSE is a relatively new technology, the development of simulative models is very useful for studying the relationship between the parameters and the physics of the process. For this reason, several researchers have developed simulative models using different software.

The thermal, mechanical, and microstructural behaviour of FSEed magnesium chips were analysed using ABAQUS software. The authors demonstrated that the rotational speed of the tool influenced the quantity of heat exchanged more than the descent feed of the tool [5].

A more focused thermal model was built using ANSYS FLUENT, in which only a linear heat flux was considered. This model proved to be able to efficiently simulate the temperature trend reached during an FSE process of a AA6061 cylinder [6].

It is worth noting that almost no model is actually able to predict the integrity of the Friction Stir Extruded products using a unique FEM model considering both the thermal and stress conditions reached during the FSE process [7]. Due to this lack of knowledge, it is important to consider other numerical models to be embedded in the simulation models. One such model is the Piwnik and Plata criterion [8]. This model, traditionally considered suitable for traditional extrusion processes but compatible with the FSE process [9], enables the evaluation of the effectiveness of the FSE process by considering the internal stress generated during the extrusion process.

The purpose of this study is to assess the feasibility of using FSE technology not only for the extrusion of solid rods but also for pipes, taking advantage of the dual configuration of direct and inverse frictional extrusion. To do that, the focus will be on two different process setups and on the extrusion of both rods and pipes. The traditional setup will be considered, in which the tool rotates and advances while the chamber remains stationary, as well as a new setup in which the tool only has an advance feed while the rotation is performed by the bottom of the chamber. Additionally, for each combination of process parameters and setups, the analysis will consider if and how the bonding phenomena occur, considering both the thermal and stress conditions generated by the parameters. For this purpose, the Piwnik and Plata criterion was chosen.

### **Materials and methods**

In order to achieve the investigation of the thermo-mechanical properties of the simulated processes, the implicit Lagrangian 3D simulation software DEFORM 3D was used. To create the simulation model, four distinct objects were taken into account: a tool, a hollow chamber, a bottom, and the material to be extruded.

The first three components were simulated as rigid objects with meshes consisting of 20,000, 27,000, and 8,000 elements, respectively. Meshes were also assigned to the rigid bodies to allow for thermal analysis of the components during the process. With regard to the material to be extruded, even though it was composed of metal shavings, it was included in the simulation model as a single porous object consisting of 61,000 tetrahedral elements. A complete representation of the model setup can be seen in Fig. 1.

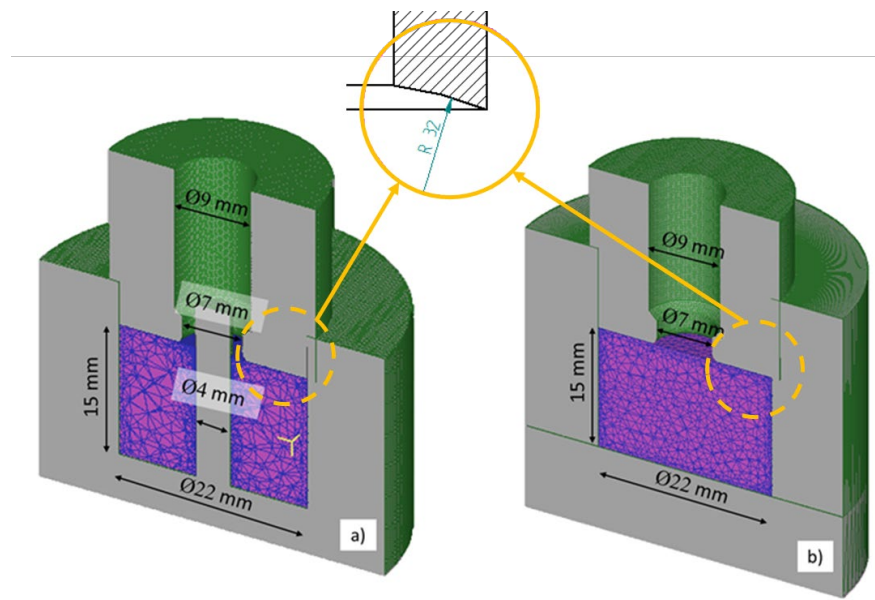


Fig. 1. Models setup for pipes (a) and for rods (b).

This choice was justified by the possibility to pre-compact the metal shavings, demonstrated in previous experimental tests, resulting in a single cylinder with a density of 2.11 g/cm<sup>3</sup>, which is 78% of the density of the base aluminium [9]. Additionally, the AISI 1043 material was assigned to the rigid bodies, while the porous workpiece was assigned AA6061 Machining-Johnson aluminium, whose mechanical properties are defined between 20°C and 550°C.

For both the direct and inverse extrusion processes, the setups reported in Fig. 1 were used. In the case of inverse extrusion, the chamber and the bottom remained static while the tool had a rotational and translational movement. Conversely, in direct extrusion modelling, the camera and the tool were kept fixed, and the bottom underwent both a translational movement along Z and a rotational motion.

The simulations were carried out by varying two parameters, namely the rotational speed (S) and vertical feed (F) of the tool/bottom, considering ranges already optimized in a previous work [9] and further analysis conducted by the authors. These parameters were both tested at two levels, as illustrated in Table 1.

**Table 1.** Process parameters combinations.

Combination	S [rpm]	F [mm/s]
1	400	1
2	400	3
3	800	1
4	800	3

To accurately capture the steady state condition of the processed material, the stop criterion for displacement in the Z direction was set at 5 mm for the primary die (either the tool for the inverse extrusion or the bottom for the direct one).

The thermal behaviour of aluminium and steel was held constant throughout all simulations, using the values presented in Table 2, which had been optimized in a prior study [9].

**Table 2.** Boundaries parameters for aluminum and steel.

Parameter	Value
Heat transfer coefficient aluminum-tool [N/s/mm/°C]	11.00
Heat exchange with the environment [N/s/mm/°C]	0.02
Thermal conductivity [N/(s·°C)]	450.00
Steel emissivity	0.70
Aluminum emissivity	0.25
Mechanical conversion to heat	0.80
Friction coefficient aluminum-tool	0.60

Previous researches in literature have demonstrated that relying solely on thermal analysis or density verification at the end of the FSE process is insufficient to ensure the successful extrusion of large pieces [9]. Therefore, it has been chosen to consider necessary to assess the internal stress state of the workpiece using the Piwnik and Plata criterion. According to this criterion, material bonding occurs when the parameter  $w$  exceeds a limit value ( $w_{lim}$ ), which is determined based on temperature. The parameter  $w$  is defined as the time integral of the ratio of pressure ( $p$ ) and the actual stress acting on the material ( $\sigma_{eff}$ ), as shown in Eq. 1:

$$w = \int_0^t \frac{p}{\sigma_{eff}} \cdot dt \tag{1}$$

To account for each step of the simulations, Eq. 1 needs to be revised as the total sum presented in Eq. 2:

$$w_{i,n} = \sum_{j=1}^n \left( \frac{p}{\sigma_{eff}} \right)_{i,j} \cdot \Delta t_j \tag{2}$$

With  $n$  = total number of steps,  $j$  = generic  $j$ -th step,  $i$  = generic  $i$ -th node and  $\Delta t_j$  = time per step of the  $j$ -th step.

For the Friction Stir Extrusion simulations, the pressure ( $p$ ) in Eq. 1 and 2 was substituted with  $\sigma_{mean}$ , which represents the average stress acting in the porous material. This choice was made because the workpiece was modelled as a single porous material, making it impossible to calculate the local pressure resulting from interactions between individual chips.

E. Ceretti et al. developed an empirical relationship for determining  $w_{lim}$  as a function of the steady-state temperature achieved during the extrusion process [10]. However, the experimental interpolation curve presented in Eq. 3 was only validated for temperatures greater than 320°C.

$$w_{lim} = 4.9063e^{-0.0017 T} \tag{3}$$

To calculate  $w$  and  $w_{lim}$  for each node at every step, a specialized Fortran routine was developed and integrated into the simulation model, enabling their automated computation and the relationship between these two parameters.

The data on bonding conditions, torque, energy from axial thrust, and energy from rotational movement were extracted and analysed after the simulations. In addition, the total energy expenditure for machining was calculated by adding the energy from axial thrust and the energy required for rotational movement, calculated as reported in Eq. 4.

$$E_r = \omega \cdot \int_0^t C dt \tag{4}$$

With  $E_r$  = energy required for rotational movement,  $\omega$  = rotational speed [rad/s],  $C$  = torque and  $t$  = time per step.

### Results and discussion

The implementation of a dedicated Fortran routine in the simulation models facilitated the automatic calculation of  $w$  and  $w_{lim}$  for each node and enabled the relationship between these two quantities to be embedded. The Piwnik and Plata criterion was then graphically represented by introducing a new user-variable called *welding*. This variable color-coded the elements in which  $w > w_{lim}$  as red and the regions in which  $w < w_{lim}$  as blue, allowing the effective proof of the Piwnik and Plata criterion to be easily identified.

By employing this method, it was possible to demonstrate the feasibility of using both direct and inverse FSE methods to produce sound and completely massive products, including rods and pipes. As already mentioned, it has been already demonstrated that the exclusive thermal analysis of the FSE process are not sufficient to ensure the extrusion of massive pieces [9]. In addition to this, based on the data collected through simulations, it was also possible to demonstrate that not even the verification of the final density of the workpiece can ensure the effective extrusion of massive pieces. In fact, in Fig.2 it is possible to observe that, considering the inverse extrusion with  $S=400$  rpm and  $F=3$  mm/s, although the temperature reached was on average higher than  $350^\circ\text{C}$  (Fig. 2a), the temperature at which chip welding begins, and that the density relative reached in the extruded part is equal to 1 (Fig. 2b), the bonding conditions have not been verified (Fig. 2c).

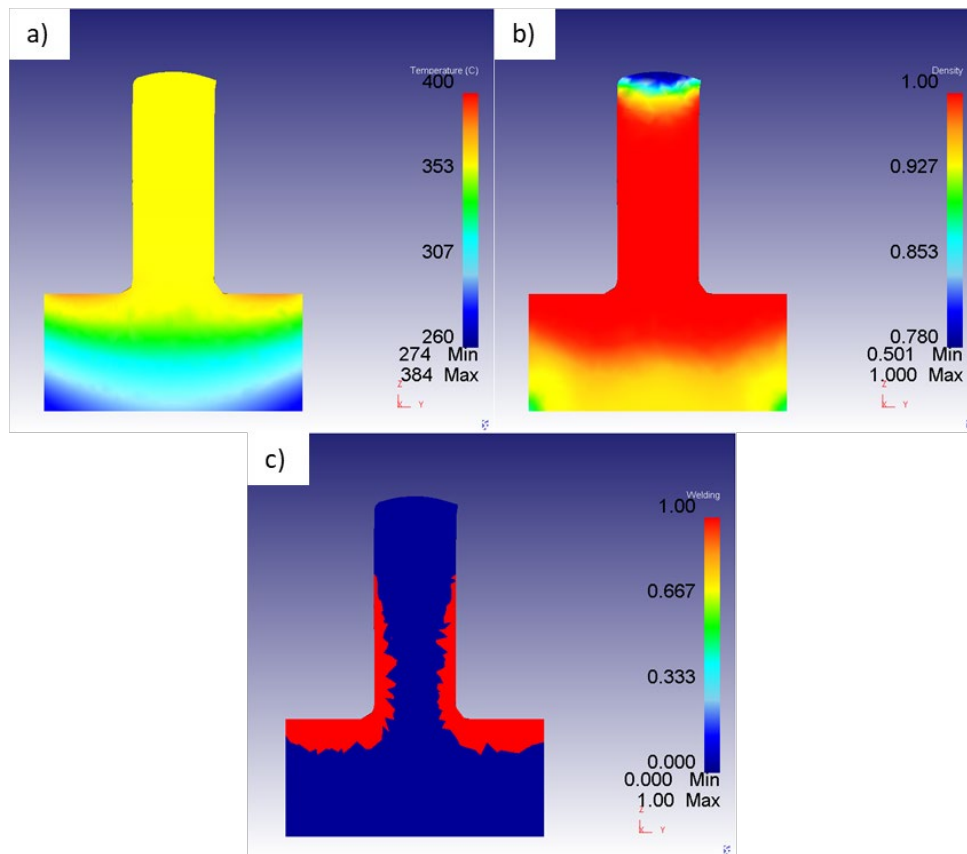


Fig. 2. FEM results: a) Temperature, b) density and c) welding parameter.

By way of example, Fig. 3 illustrates the outcome obtained by considering the direct extrusion of a pipe with  $S=800$  rpm and  $F=1$  mm/s, which enabled both extruded geometries to be produced.

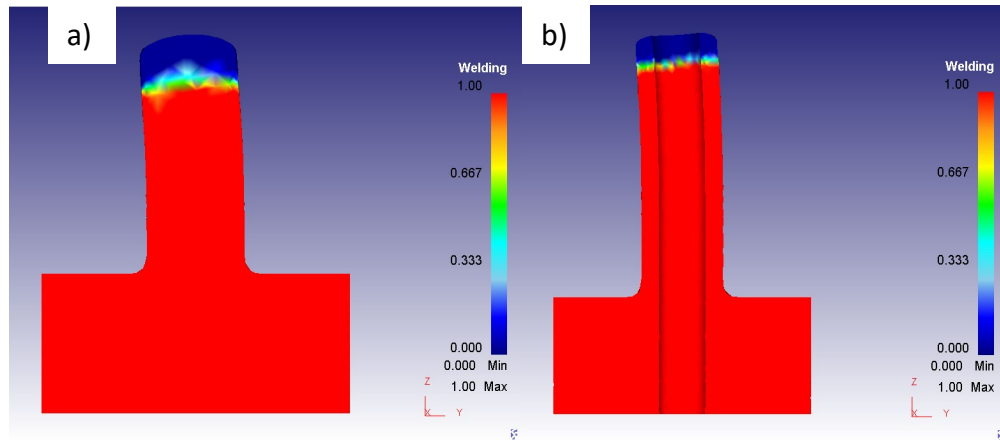


Fig. 3. FEM results obtained: a) rod with direct extrusion and b) pipe with inverse FSE process.

The torque resulting from the different simulations are reported in Fig. 4 and Fig. 5.

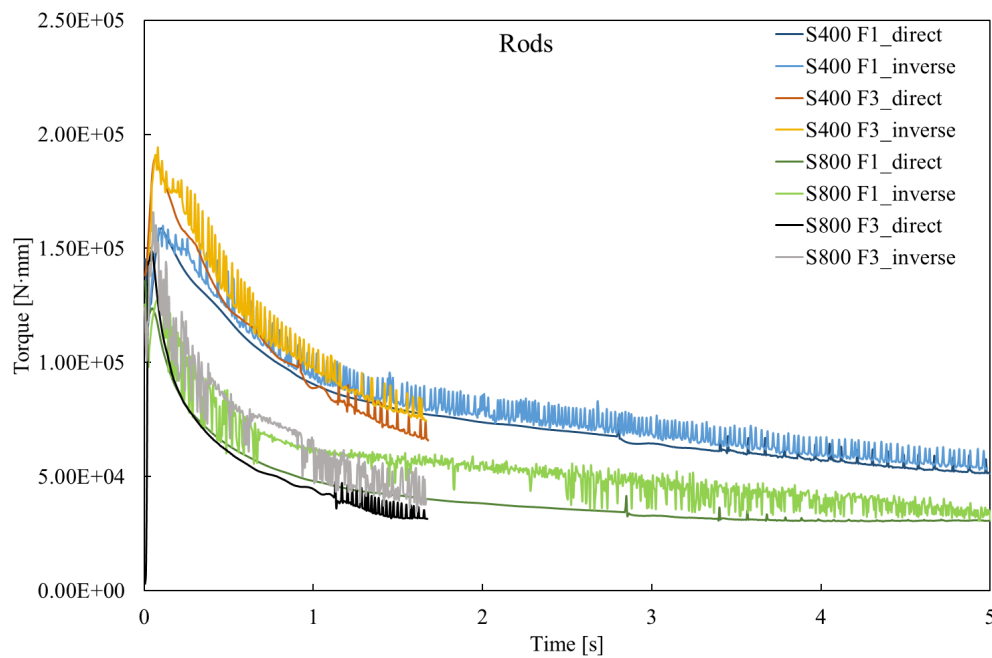


Fig. 4. Torque results from the direct and inverse FSE simulation of rods.

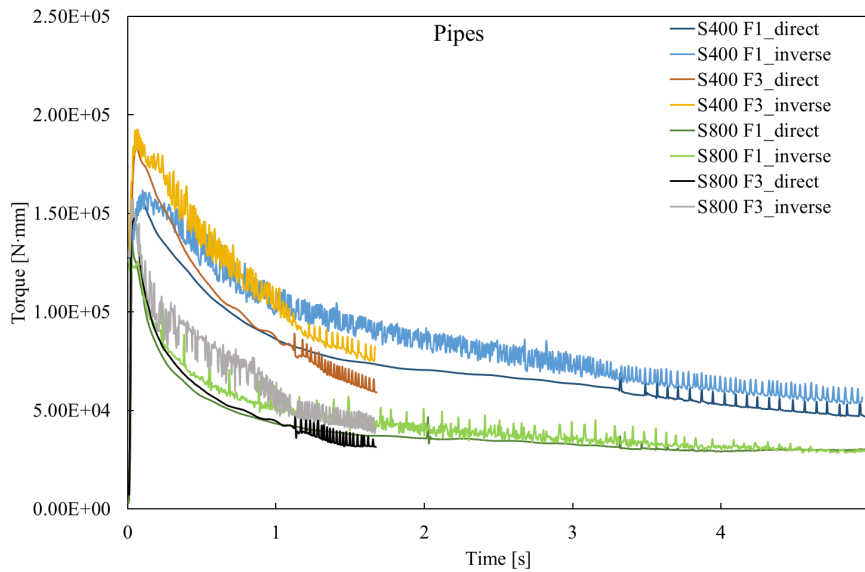


Fig. 5. Torque results from the direct and inverse FSE simulation of pipes.

Starting from these results, by using the Eq. 4, the  $E_r$  was calculated for each combination of process parameters. This energy component was added to the energy demand resulted directly from the Deform post-processor, obtaining the total energy demand ( $E_{tot}$ ).

In Table 3 all the results of the bonding occurrence as a function of both the process parameters and the calculated energy demands are reported. The cells corresponding to the conditions in which perfect bonding was found are highlighted in green, in red where there was no bonding.

Table 3. Simulation results of the energy demands.

S [rpm]	F [mm/s]	Direct extrusion		Inverse extrusion	
		Rods	Pipes	Rods	Pipes
		$E_{tot}$ [KJ]	$E_{tot}$ [KJ]	$E_{tot}$ [KJ]	$E_{tot}$ [KJ]
400	1	16.82	16.15	17.61	18.45
400	3	8.56	8.27	8.81	9.03
800	1	18.2	17.25	22.94	18.92
800	3	8.39	8.37	10.73	10.06

The differences between the direct and inverse extrusion configurations in terms of energy, with the same process parameters, are almost negligible.

However, it immediately became clear that, with the same energy demand -or even lower-, with direct extrusion it was possible to obtain massive pieces also considering the pairs of parameters which did not lead to bonding in the inverse extrusion.

This is due to the benefit of the direct FSE which lies in complete compaction of the chips before the start of extrusion inside the tool cavity. This led to a more thermally uniform starting workpiece, which was ready for fully compacted material extrusion. As a result, the forces required at the interface between the tool and the workpiece were reduced, allowing for bonding even at lower temperatures and creating a state of stress that facilitated the production of completely massive pieces.

### Conclusions

The objective of this study is to assess the feasibility of using FSE technology for direct and inverse extrusion of fully dense rods and pipes, by analysing bonding conditions through the Piwnik and

Plata criterion. A robust FEM model was developed to consider the rotational and descent speeds of the tool/bottom, and determine a reliable technology window for FSE. The study demonstrates that both direct and inverse extrusion configurations can be employed, and full dense rods and pipes can be produced with both configurations. Furthermore, it seems that the direct FSE provides a better starting point for the active extrusion phase, allowing the reduction of the energy consumption and limiting, at the same time, the non-bonding technological window.

## References

- [1] D. Baffari, G. Buffa, D. Campanella, L. Fratini, A.P. Reynolds, Process mechanics in Friction Stir Extrusion of magnesium alloys chips through experiments and numerical simulation, *J. Manuf. Process.* 29 (2017) 41–49.
- [2] V.C. Shunmugasamy, E. Khalid, B. Mansoor, Friction stir extrusion of ultra-thin wall biodegradable magnesium alloy tubes — Microstructure and corrosion response, *Mater. Today Commun.* 26 (2021) 102129. <https://doi.org/10.1016/j.mtcomm.2021.102129>
- [3] W.T. Evans, B.T. Gibson, J.T. Reynolds, A.M. Strauss, G.E. Cook, Friction Stir Extrusion: A new process for joining dissimilar materials, *Manuf. Lett.* 5 (2015) 25–28. <https://doi.org/10.1016/j.mfglet.2015.07.001>
- [4] R.M. Izatt, *Metal Sustainability: Global Challenges, Consequences, and Prospects*, Wiley, 2016. <https://doi.org/10.1002/9781119009115>
- [5] R.A. Behnagh, N. Shen, M.A. Ansari, M. Narvan, M. Kazem, B. Givi, H. Ding, Experimental analysis and microstructure modeling of friction stir extrusion of magnesium chips, *J. Manuf. Sci. Eng. Trans. ASME.* 138 (2016). <https://doi.org/10.1115/1.4031281>
- [6] H. Zhang, X. Li, W. Tang, X. Deng, A.P. Reynolds, M.A. Sutton, Heat transfer modeling of the friction extrusion process, *J. Mater. Process. Technol.* 221 (2015) 21–30. <https://doi.org/10.1016/j.jmatprotec.2015.01.032>
- [7] D. Baffari, G. Buffa, L. Fratini, A numerical model for Wire integrity prediction in Friction Stir Extrusion of magnesium alloys, *J. Mater. Process. Technol.* 247 (2017) 1–10. <https://doi.org/10.1016/j.jmatprotec.2017.04.007>
- [8] M. Plata, J. Piwnik, Theoretical and experimental analysis of seam weld formation in hot extrusion of aluminum alloys, in: *7th Int. Alum. Extrus. Technol.*, 2000: pp. 205–211.
- [9] S. Bocchi, G. D’urso, C. Giardini, G. Maccarini, A Simulative Method for Studying the Bonding Condition of Friction Stir Extrusion, *Key Eng. Mater.* 926 KEM (2022) 2333–2341. <https://doi.org/10.4028/P-FT5355>
- [10] E. Ceretti, L. Fratini, F. Gagliardi, C. Giardini, A new approach to study material bonding in extrusion porthole dies, *CIRP Ann. - Manuf. Technol.* 58 (2009) 259–262. <https://doi.org/10.1016/j.cirp.2009.03.010>